

Crystal Structures and Physical Properties of 1,6-Diaminopyrene-*p*-chloranil (DAP-CHL) Charge-Transfer Complex. Two Polymorphs and Their Unusual Electrical Properties

Hirotohi Goto, Tasuku Fujinawa, Hidemasa Asahi, Tamotsu Inabe,* Hironori Ogata,†

Seiichi Miyajima,† and Yusei Maruyama†

Department of Chemistry, Faculty of Science, Hokkaido University, Sapporo 060

†Institute for Molecular Science, Myodaiji, Okazaki 444

(Received August 21, 1995)

A combination of 1,6-diaminopyrene and *p*-chloranil gives two kinds of 1 : 1 charge-transfer complex crystals from a benzene solution. The α -form is triclinic, space group $P\bar{1}$, $a = 8.963(1)$, $b = 9.112(2)$, $c = 6.730(1)$ Å, $\alpha = 99.59(1)$, $\beta = 99.65(1)$, $\gamma = 114.43(1)^\circ$, $V = 476.0(1)$ Å³, and $Z = 1$; the β -form is also triclinic, space group $P\bar{1}$, $a = 8.123(3)$, $b = 9.708(3)$, $c = 6.791(2)$ Å, $\alpha = 110.73(2)$, $\beta = 108.89(2)$, $\gamma = 79.11(3)^\circ$, $V = 472.3(3)$ Å³, and $Z = 1$. In both crystals, the donors and acceptors are neutral, and stack alternately. The main difference between the α - and β -forms is in the overlapping mode. Both crystals are electrically insulating at the initial states. The α -form single crystal, however, undergoes and irreversible conductivity change upon mild heating (< 380 K) or fracture of the crystal into powder. In both cases, the conductivity change amounts to 10^6 to 10^8 , and the resultant solids are highly conducting semiconductors. Structural, optical, magnetic, and solid-state NMR studies suggest that the low-resistance state mainly comprises neutral molecules, despite its high conductivity. The resistivity of β -DAP-CHL also decreases upon heating to above 400 K, while fracture of the crystal has no effects. The resistivity change in β -DAP-CHL is considered as simple ionization of a part of the components.

After the discovery of highly conducting TCNQ (α, α', α' -tetracyanoquinodimethane) complexes, the search for other organic conductors has successfully progressed, and the guidelines for constructing organic conductors now seem to be established. For combining a donor and an acceptor, one must consider the difference between the oxidation potential of the donor and the reduction potential of the acceptor,¹⁾ as well as the symmetry of the HOMO of the donor and the LUMO of the acceptor.²⁾ The former is related to a requirement for realizing a partial charge transfer, and the latter is related to another requirement for realizing the segregated stacking of donors and acceptors. When the second requirement is not achieved, i.e., donors and acceptors make mixed-stack columns, the complex is not a metallic conductor. Some complexes which fulfill only the first requirement show relatively high conductivities, despite the mixed stacking structure, though they are always semiconductors.

The title complex, 1,6-diaminopyrene-*p*-chloranil (DAP-CHL), is one of the very early organic semiconductors (Chart 1). A resistivity of $4 \times 10^3 \Omega \text{ cm}$ for a compressed pellet was reported in 1961.³⁾ At the early stage, this relatively low resistivity was attributed to the ionized components,⁴⁾ like other conducting complexes related to the first requirement mentioned above. Shortly later, it was, however, found that the components are not ionized in the complex, and it was recognized that the electrical properties of this complex

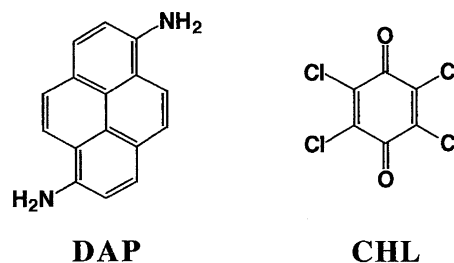


Chart 1.

are not consistent with its electronic state.⁵⁾ Subsequent studies found that there exist polymorphic forms, and that one of them (green form) has a high resistivity, which is consistent with the neutral ground state of the complex.^{6,7)} However, this study raised another question; the resistivity of another form (brown form) is varied by the preparation procedure of the compressed pellet. After these studies, DAP-CHL has not been subjected to further studies.

We have been interested in this complex from a different point of view. We have already proposed that a kind of proton-electron cooperation in charge-transfer complexes may be utilized to design novel molecular devices.⁸⁾ As a candidate of an intermolecular hydrogen-bonded system, charge-transfer complexes of DAP have been selected, because the amino groups in DAP are feasible to form hydrogen bonds with a wide variety of benzoquinone-type and TCNQ-type

acceptors. Recently, we reported that DAP-TCNQ, which crystallizes with segregated stacks of donors and acceptors, is highly conductive, but the activation energy for the conduction is extremely high over a wide temperature range.⁹⁾ Though it is not yet clear whether this unusual property is directly related to the hydrogen bond or not, it is worthwhile examining the crystal structures and properties of other hydrogen-bonded DAP complexes. In this paper we describe a drastic conductivity change upon a heat treatment or fracture of the crystals of DAP-CHL, which was found during the course of our study of DAP complexes.

Experimental

Materials. DAP was synthesized following a method reported in the literature,¹⁰⁾ and was carefully purified by repeated treatments with sulfuric acid followed by recrystallization and vacuum sublimation. When the purification was not sufficient, a trace amount of isomer, 1,8-diaminopyrene, seriously affected the crystal quality of DAP-CHL.¹¹⁾ CHL was commercially obtained and purified by recrystallization followed by vacuum sublimation. Single crystals of DAP-CHL were grown by slow cooling and prolonged slow evaporation of the benzene solution. Two polymorphs were obtained from the same solution, and were easily distinguishable from their appearances; obtained dark-brown and dark-green crystals corresponded to the brown and green forms in Ref. 6, respectively, and hereafter are called α - and β -forms, respectively.

Measurements. Electrical conductivity measurements were performed by a four-probe method for low-resistance samples and a two-probe method for high-resistance samples. The infrared spectra of single-crystal specimens were recorded on a Perkin-Elmer 1650 FT-IR microscope system. ESR experiments were performed with using a JEOL JES-FE1X spectrometer. Magnetic-susceptibility measurements were carried out using a Quantum Design MPMS SQUID susceptometer.

Solid-state high-resolution ¹³C NMR was conducted with a JEOL GSX-270 spectrometer working at 68 MHz. A cross-polarization/magic-angle sample spinning (CP/MAS) method¹²⁾ was applied with a contact time of 5 ms and a spinning frequency of 3.8 kHz. The chemical shift was measured with respect to liquid tetramethylsilane (TMS). Typically, the spectral resolution was 5 Hz for solid adamantane. Powdered hexamethylbenzene (HMB) was added to the sample as an internal standard in order to evaluate any subtle change in the chemical shift. A solid-state high-resolution ¹H NMR experiment was carried out using a Bruker ASX-300 spectrometer at 300 MHz. A CRAMPS (combined rotation and a multiple-pulse spectroscopy) method¹²⁾ was applied with sample rotation of 1.5 kHz and MREV-8 pulse sequence. Tetrakis(trimethylsilyl)silane (TTMS) powder was added as an internal shift standard (+0.247 ppm with respect to TMS). The spectral resolution was checked by glycine; two methylene peaks were resolved, with a half-value width of ca. 300 Hz for each. Scaling in the frequency domain was achieved by observing the water signal. All of the NMR experiments were performed at room temperature by using polycrystalline (high-resistance α -DAP-CHL) and compressed-powder (low-resistance α -DAP-CHL) specimens.

X-Ray Structure Analyses. An automated Rigaku AFC-5R diffractometer with graphite monochromatized Mo K α radiation ($\lambda = 0.71073$ Å) was used for data collection at room temperature for pristine and low-resistance α -DAP-CHL, and β -DAP-CHL. The data-collection conditions are summarized in Table 1. Three standard reflections, which were monitored every 100 or 150 data

measurements, showed no significant deviation in intensities.

The crystal structures were solved by the Patterson method (α -DAP-CHL) and a direct method¹³⁾ (β -DAP-CHL), and the positions of all the hydrogen atoms were determined from difference synthesis maps. A block-diagonal least-squares technique (UNICS III¹⁴⁾) with anisotropic thermal parameters for non-hydrogen atoms and isotropic for hydrogen atoms was employed for the structure refinement.

Results and Discussion

Crystal Structure of α -DAP-CHL. The molecular structures of DAP and CHL in α -DAP-CHL determined from an analysis of the X-ray diffraction data is shown in Fig. 1, and the atomic parameters are given in Table 2.¹⁵⁾ The bond lengths for pristine α -DAP-CHL are compiled in Table 3 together with those for β -DAP-CHL and low-resistance α -DAP-CHL (vide infra). Quinonoid-type acceptors are known to change the bond lengths upon accepting an electron; a quinonoid-type framework changes to a semiquinone-type framework. Therefore, the bond lengths are believed to be an index of the degree of ionization. In the case of CHL, clear changes in the bond lengths can be seen from a comparison of the bond lengths between CHL¹⁶⁾ and K⁺CHL⁻¹⁷⁾ (Table 4). When the mean bond lengths observed for pristine α -DAP-CHL are compared with those values, one can definitely judge that CHL is completely neutral. However, this fact is rather curious, since the ionization potential of DAP is very low. The first oxidation potential, E_{ox} ($E = (E^a + E^c)/2$, where E^a and E^c are anodic and cathodic peak potentials, respectively), of DAP is 0.24 V vs. Ag/AgCl in acetonitrile using Bu₄N⁺BF₄⁻ as an electrolyte. Thus, the difference between the electrochemical oxidation potential of DAP and the reduction potential of CHL ($E_{red} = -0.02$ V under the same conditions), $\Delta E_{redox} = E_{ox} - E_{red}$, is only 0.26 V, suggesting that the ground state of this complex situates in the ionic region, or very close to the ionic-neutral boundary.¹⁸⁾

The crystal structure of α -DAP-CHL is shown in Fig. 2. The donors and acceptors are located on the inversion centers and form mixed-stacks along the *c*-axis with an interplanar spacing of 3.35 Å. The hydrogen bonds between the amino group of DAP and the carbonyl oxygen of CHL are formed along the [221] direction. Therefore, the molecules are bound in a two-dimensional sheet parallel to the (1 $\bar{1}$ 0) plane. The hydrogen-bonded N...O distance is not very

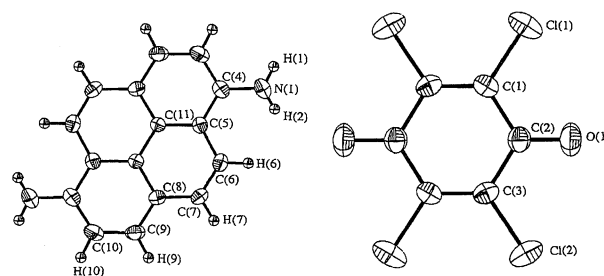


Fig. 1. ORTEP drawing of DAP and CHL in pristine α -DAP-CHL showing the atom numbering scheme. The scheme is common for β -DAP-CHL and low-resistance α -DAP-CHL.

Table 1. Data-Collection Conditions and Crystal Data

	Pristine α -DAP-CHL	Low-resistance α -DAP-CHL	β -DAP-CHL
Chemical formula	C ₂₂ H ₁₂ Cl ₄ N ₂ O ₂	C ₂₂ H ₁₂ Cl ₄ N ₂ O ₂	C ₂₂ H ₁₂ Cl ₄ N ₂ O ₂
Molecular weight	478.16	478.16	478.16
Crystal system	Triclinic	Triclinic	Triclinic
Space group	$P\bar{1}$	$P\bar{1}$	$P\bar{1}$
$a/\text{\AA}$	8.963(1)	8.962(2)	8.123(3)
$b/\text{\AA}$	9.112(2)	9.113(2)	9.708(3)
$c/\text{\AA}$	6.730(1)	6.730(1)	6.791(2)
α/deg	99.59(1)	99.59(2)	110.73(2)
β/deg	99.65(1)	99.65(2)	108.89(2)
γ/deg	114.43(1)	114.43(2)	79.11(3)
$V/\text{\AA}^3$	476.0(1)	476.0(2)	472.3(3)
Z	1	1	1
$D_{\text{calcd}}/\text{g cm}^{-3}$	1.668	1.668	1.681
$\mu(\text{Mo } K\alpha)/\text{cm}^{-1}$	6.47	6.47	6.52
2θ range	$5^\circ < 2\theta < 60^\circ$	$5^\circ < 2\theta < 60^\circ$	$2^\circ < 2\theta < 60^\circ$
Range of h, k , and l	$0 \leq h \leq 12$ $-12 \leq k \leq 11$ $-9 \leq l \leq 8$	$0 \leq h \leq 12$ $-12 \leq k \leq 11$ $-9 \leq l \leq 8$	$-11 \leq h \leq 11$ $-14 \leq k \leq 14$ $0 \leq l \leq 10$
Scan width/deg	$1.5+0.3 \tan \theta$	$1.57+0.3 \tan \theta$	$1.2+0.5 \tan \theta$
Scan mode	$\omega-2\theta$	$\omega-2\theta$	$\omega-2\theta$
Scan rate/deg min ⁻¹	6	6	3
Number of reflections measured	2943	2944	2976
Number of independent reflections observed ($F_o > 3\sigma(F_o)$)	2423	1970	1833
Number of parameters	161	161	161
R	0.040	0.044	0.042
R_w	0.050	0.042	0.033
Weighting factor (g) $w^{-1} = \sigma^2 + (gF)^2$	0.015	0.015	0.015

Table 2. Fractional Coordinates ($\times 10^4$) and Equivalent Temperature Factors for pristine α -DAP-CHL

Atom	x	y	z	$B_{\text{eq}}/\text{\AA}^2$ a)
Cl(1)	-1034(1)	2910(1)	371(1)	4.78(1)
Cl(2)	-3867(1)	-907(1)	-1125(1)	4.41(1)
O(1)	2352(2)	3162(1)	1230(2)	4.17(4)
C(1)	-558(2)	1272(2)	140(2)	2.90(4)
C(2)	1281(2)	1725(2)	673(2)	2.82(4)
C(3)	-1745(2)	-323(2)	-487(2)	2.83(4)
N(1)	5421(2)	3025(2)	-3045(3)	4.44(5)
C(4)	3740(2)	2734(2)	-3487(2)	3.05(4)
C(5)	2401(2)	1084(2)	-4175(2)	2.55(4)
C(6)	2707(2)	-355(2)	-4429(2)	3.02(4)
C(7)	1409(2)	-1920(2)	-5079(2)	3.11(4)
C(8)	-327(2)	-2222(2)	-5547(2)	2.67(4)
C(9)	-1694(2)	-3826(2)	-6202(3)	3.39(4)
C(10)	-3351(2)	-4075(2)	-6664(3)	3.53(4)
C(11)	689(2)	830(2)	-4657(2)	2.25(3)

$$a) B_{\text{eq}} = 4/3 \sum_i \sum_j \beta_{ij} a_i \cdot a_j.$$

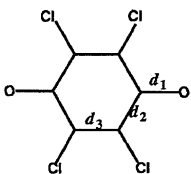
Table 3. Bond Distances of DAP-CHL (\AA)

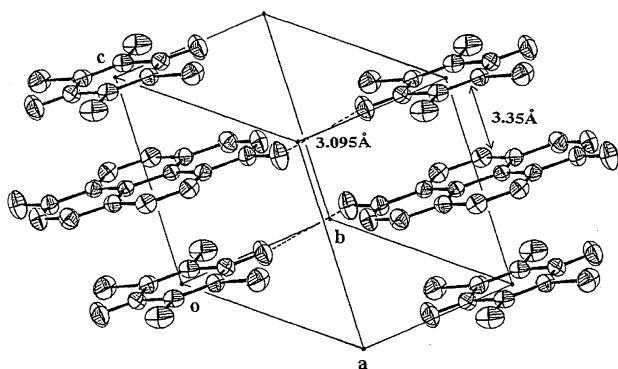
Bond	Pristine α -DAP-CHL	Low-resistance α -DAP-CHL	β -DAP-CHL
Cl(1)-C(1)	1.705(2)	1.708(3)	1.705(2)
Cl(2)-C(3)	1.703(2)	1.703(2)	1.711(2)
O(1)-C(2)	1.206(2)	1.202(2)	1.215(2)
C(1)-C(2)	1.486(2)	1.483(3)	1.486(2)
C(1)-C(3)	1.337(2)	1.336(3)	1.342(3)
C(2)-C(3)	1.491(3)	1.496(4)	1.487(3)
N(1)-C(4)	1.387(2)	1.384(3)	1.386(3)
C(4)-C(5)	1.415(2)	1.419(2)	1.416(3)
C(4)-C(10)	1.396(3)	1.396(4)	1.398(3)
C(5)-C(6)	1.436(3)	1.437(4)	1.428(2)
C(5)-C(11)	1.424(2)	1.423(3)	1.427(2)
C(6)-C(7)	1.352(2)	1.344(3)	1.352(3)
C(7)-C(8)	1.431(2)	1.428(3)	1.430(3)
C(8)-C(9)	1.398(2)	1.402(2)	1.397(3)
C(8)-C(11)	1.425(2)	1.425(4)	1.419(3)
C(9)-C(10)	1.377(3)	1.374(4)	1.377(3)
C(11)-C(11')	1.435(1)	1.436(2)	1.429(2)

short; the value, 3.095(2) \AA , is only slightly shorter than the sum of the van der Waals radii (3.10 \AA). When the purification of DAP was not sufficient, stacking faults between

the sheets were observed.¹¹⁾ The existence of structural defects, however, does not affect the transport properties. In

Table 4. Comparison of Bond Lengths in CHL

			
Compound	$d_1/\text{\AA}$	$d_2/\text{\AA}$	$d_3/\text{\AA}$
CHL	1.211(2)	1.490(2)	1.344(2)
K^+CHL^-	1.26(2)	1.44(2)	1.37(2)
Pristine α -DAP-CHL	1.206(2)	1.489(3)	1.337(2)
Low-resistance α -DAP-CHL	1.202(2)	1.490(7)	1.336(3)
β -DAP-CHL	1.215(2)	1.487(3)	1.341(2)

Fig. 2. Crystal structure of pristine α -DAP-CHL.

the present study, all of the crystals used for the structural and transport measurements were of high quality.

Electrical Resistivity of α -DAP-CHL. The electrical resistivity of the pristine crystal is high ($10^8 \Omega \text{ cm}$ at room temperature). This is consistent with the neutral ground state of this complex evaluated from the molecular geometry of CHL.

When the resistivity along the c -axis of a single crystal was measured with increasing the temperature, a drastic conductivity change was observed. Two examples are shown in Fig. 3. The temperature at which point the resistivity drops abruptly is not the same for all the crystals; some crystals become low-resistance state at relatively low temperature, while some others persist in the high-resistance state near to 380 K. In any case, the resistivity drop occurs directly, though some crystals show a multi-step change. It is common for all the crystals that the low-resistance state does not return to the high-resistance state after cooling. The effect of oxygen was checked with the measurements under different conditions, namely in vacuum, in 1 atm He gas, in 1 atm O_2 gas, and in air. The behavior was essentially independent on these conditions.

It was also found that the resistivity of pristine α -DAP-CHL was dramatically decreased by compression of the single crystals into a pellet. Since the resistivity changes at a relatively low applied pressure, and is almost independent of

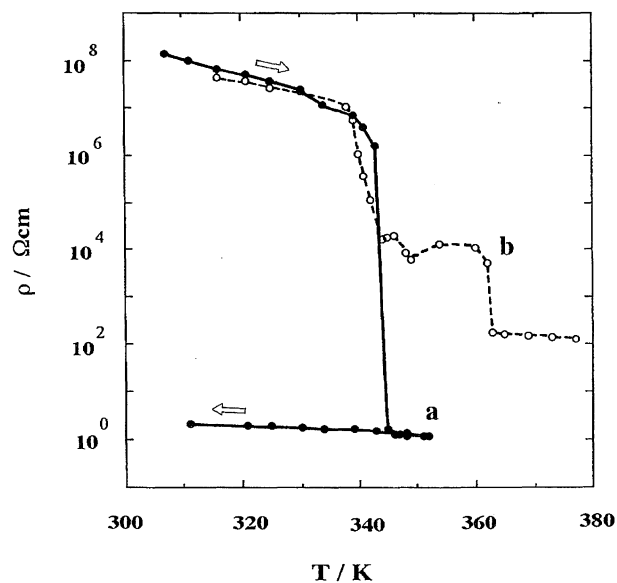


Fig. 3. Electrical resistivity of α -DAP-CHL single crystals. **a** and **b** are independent runs for the different crystals and arrows are the direction of the temperature change.

the applied pressure, this change is considered to result from mechanical crushing of the crystals. The resistivity is almost comparable to those values of single crystals transformed into the low-resistance state by a heat treatment, as shown in Fig. 4. This suggests that the anisotropy of conduction must be small. In fact, the anisotropy, $\rho_{\perp c}/\rho_{\parallel c}$,¹⁹⁾ has been found to be less than 10 by measurements using single crystals.

Comparison between Pristine α -DAP-CHL and Low-Resistance α -DAP-CHL.

The appearance of the crystals in the low-resistance state is not different from that of pristine crystals. The crystal, which is transformed into the low-resistance state at relatively low temperature, is actually applicable to a single-crystal X-ray diffraction study. The obtained atomic parameters are tabulated in Table 5. As can be seen from Tables 1, 3, and 4, the molecular and crystal structures derived from the diffraction data of low-resistance

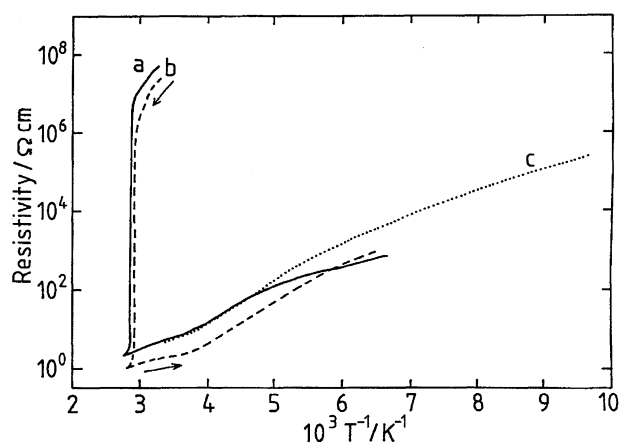


Fig. 4. Temperature dependence of the electrical resistivity of α -DAP-CHL; single crystals, **a** and **b**, and powder compaction pressed at 71 kg cm^{-2} , **c**.

Table 5. Fractional Coordinates ($\times 10^4$) and Equivalent Temperature Factors for Low-Resistance α -DAP-CHL

Atom	<i>x</i>	<i>y</i>	<i>z</i>	<i>B</i> _{eq} /Å ² a)
Cl(1)	−1034(1)	2910(1)	372(1)	4.70(2)
Cl(2)	−3869(1)	−908(1)	−1126(1)	4.30(2)
O(1)	2352(2)	3161(2)	1230(3)	4.1(1)
C(1)	−558(3)	1269(2)	133(3)	2.9(1)
C(2)	1280(3)	1729(2)	677(3)	2.7(1)
C(3)	−1745(2)	−323(2)	−491(3)	2.6(1)
N(1)	5417(2)	3022(3)	−3042(3)	4.3(1)
C(4)	3739(3)	2734(3)	−3487(3)	2.9(1)
C(5)	2397(2)	1080(2)	−4178(3)	2.5(1)
C(6)	2698(3)	−363(3)	−4430(3)	3.0(1)
C(7)	1408(3)	−1918(3)	−5079(3)	3.1(1)
C(8)	−325(3)	−2223(2)	−5549(3)	2.6(1)
C(9)	−1697(3)	−3830(3)	−6201(3)	3.2(1)
C(10)	−3350(3)	−4075(3)	−6667(3)	3.4(1)
C(11)	688(2)	832(2)	−4656(3)	2.2(1)

$$a) B_{eq} = 4/3 \sum_i \sum_j \beta_{ij} a_i \cdot a_j.$$

α -DAP-CHL are essentially the same as those in pristine α -DAP-CHL. The geometry of CHL therefore indicates that the molecule is neutral.

Figure 5 shows the infrared spectra of single-crystal DAP-CHL. In the high-resistance phase, the peaks correspond well to those of the neutral components. When the crystal is transformed into the low-resistance phase, appreciable growth of the electronic absorption in the infrared region is noticed. The vibrational bands are, however, observed exactly at the same frequencies. The spectrum of the powdered specimen is basically the same; it consists of broad electronic absorption bands and vibrational bands of neutral components. These facts indicate that the components are neutral in both phases, and are consistent with the results of an X-ray analysis.

The above results are very mysterious, since the resistivity is unusually low as a complex with a neutral ground state. This point was checked by ESR measurements. The ESR signal of a pristine crystals is quite weak, indicating very low concentration of the ionized species (probably defects). When the temperature is increased, the intensity of the signal suddenly becomes larger at nearly the same temperature region where the resistivity drop was observed. The temperature dependence of the signal intensity of the low-resistance phase is shown in Fig. 6. The behavior is essentially common for compressed pellets and single crystals; the intensity is gradually decreased with decreasing temperature until 200 K. The susceptibility of pristine α -DAP-CHL measured by a SQUID susceptometer consists of only a small amount of a Curie-type paramagnetic component (0.04%) besides the diamagnetic core contribution. The susceptibility of low-resistance α -DAP-CHL was measured using a compressed pellet. As found in the ESR measurements, a slight increase in the paramagnetic components was observed. The temperature dependence is shown in Fig. 7, in which a small susceptibility range is expanded in order to clarify the change.

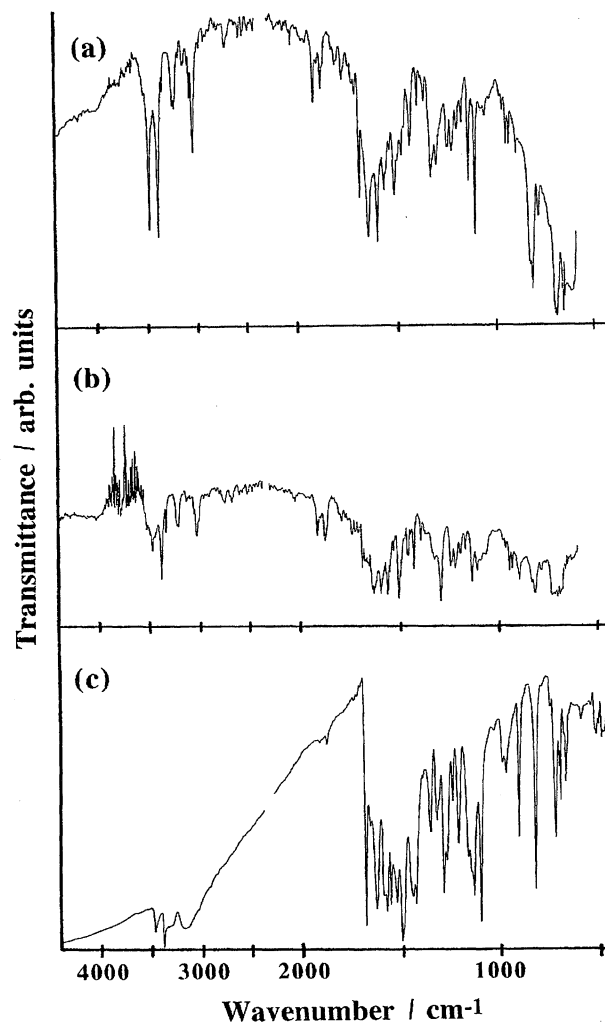


Fig. 5. Infrared spectra of α -DAP-CHL; pristine single crystal (a), low-resistance single crystal (b), and the powder in the form of KBr disc (c).

The temperature-dependent susceptibility at low temperatures seems to be a Curie-type component. Above 200 K, there seems to be another component which increases with increasing the temperature. Thus, the fitting was attempted by

$$\chi = A + \frac{B}{T} + \frac{C}{T} \left\{ \frac{4 \exp\left(-\frac{2J}{kT}\right)}{1 + 3 \exp\left(-\frac{2J}{kT}\right)} \right\}, \quad (1)$$

assuming that the susceptibility is composed of a core diamagnetic component and Curie-type and singlet-triplet-type paramagnetic components. The solid line in Fig. 7 is obtained with $A = -2.74 \times 10^{-4}$ emu mol⁻¹, $B = 0.003$ emu K mol⁻¹, $C = 0.025$ emu K mol⁻¹, and $J/k = 500$ K. The diamagnetic contribution is in good agreement with the sum of the Pascal's constants (-2.67×10^{-4} emu mol⁻¹), and from the ratio of B or C and the Curie constant, the Curie-type paramagnetic component is obtained as 0.8%, and the singlet-triplet-type paramagnetic spin 1/2 pairs as about 3.3% of the donor-acceptor pairs. The number of spins (ionized molecules) is still very small, though it is increased by a transformation into

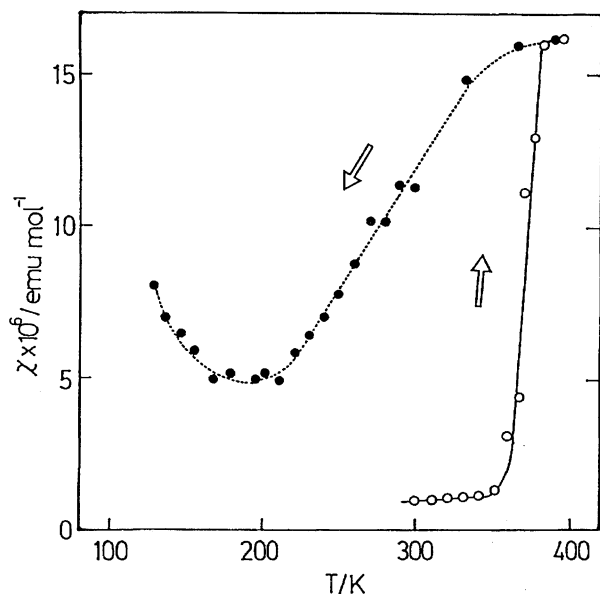


Fig. 6. Paramagnetic susceptibility of single crystal α -DAP-CHL evaluated from the ESR signal intensity. Arrows are the direction of the temperature change, and lines are a guide for eyes.

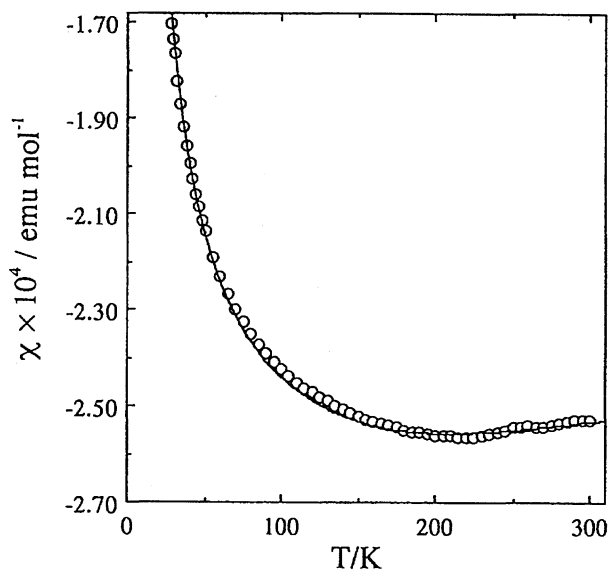


Fig. 7. Magnetic susceptibility of powder compaction of α -DAP-CHL pressed at 1500 kg cm^{-2} . Solid line is a fitting (see text).

the low-resistance state.

The simplest interpretation of all the observations discussed above is that the low-resistance state is a kind of mixture of which the majority comprises neutral molecules. In this case, electrical conduction is assumed to be achieved through the small amount of ionized parts, the existence of which cannot be detected in X-ray measurements, but can be detected by magnetic measurements. However, there still remains a question; the resistivity observed is for the total volume of the sample. If the conduction occurs through only a part of the sample, which may be 3.3% of the cross section,

the resistivity of the conductive part has to be much lower than the observed value, probably on the order of $10^{-2} \Omega \text{ cm}$. Since the transformation from the high-resistance state to the low-resistance state is easily achieved, it is not likely that this process is accompanied by a drastic structural change. It is hard to believe that a solid derived from a mixed-stack-type structure has a resistivity of $10^{-2} \Omega \text{ cm}$.

Solid-State NMR of α -DAP-CHL. Solid-state ^{13}C NMR is expected to provide information on: (i) the difference in the crystal structure between the high-resistance and low-resistance phases, (ii) the difference in the average charge-transfer rate between the two phases, (iii) the possible existence of ionic species (heterogeneous nature) in the low-resistance phase, and (iv) whether the electron spins are localized or delocalized in the low-resistance phase. Fig. 8 shows the ^{13}C NMR spectra of pristine α -DAP-CHL and low-resistance α -DAP-CHL. Only the donor region is shown. The sharp singlet peak at 132.3 ppm is due to the aromatic carbon of HMB as an internal-shift standard. The peak positions are listed in Table 6. The two phases exhibit similar spectra, and the signal region is almost the same as that of pure DAP, confirming that DAP is essentially in its neutral form in either of the two phases, and that there is no appreciable

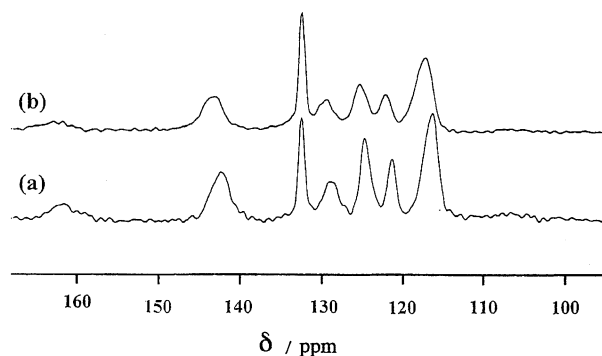


Fig. 8. CP/MAS ^{13}C NMR spectra of pristine α -DAP-CHL (a) and low-resistance α -DAP-CHL (b). Only the donor region is shown. The sharp peak at 132.3 ppm is due to the aromatic carbon of an internal shift standard (HMB).

Table 6. ^{13}C and ^1H Isotropic Chemical Shifts δ (ppm) of DAP in Pristine α -DAP-CHL and Low-Resistance α -DAP-CHL. Chemical Shifts are Measured Relative to Liquid TMS for ^{13}C and to Solid TTMS for ^1H . $\Delta\delta$ is the Difference between δ of Low-Resistance α -DAP-CHL and δ of Pristine α -DAP-CHL

Low-resistance α -DAP-CHL	Pristine α -DAP-CHL	$\Delta\delta$
^{13}C		
117.15	116.18	0.97
122.10	121.23	0.87
125.31	124.53	0.78
129.39	128.90	0.49
142.89	142.11	0.78
163	162	1
^1H		
6.5	5.8	0.7

structural transformation between the two phases. Regarding the possible heterogeneous nature of the low-resistance phase, we did not detect any additional lines, which means that the low-resistance phase is fairly homogeneous from the NMR point of view. It is remarkable that no signs of localized electron spins were detected, though the susceptibility measurement claimed the existence of a Curie component at a concentration of 0.8%.

We now analyze the difference in the two spectra in Fig. 8 in terms of the change in the electronic structure. Each of the six peaks in the low-resistance phase spectrum is slightly broadened and shifted downfield compared with the pristine phase spectrum. Table 6 shows that a downfield shift of 0.49–1 ppm takes place nearly independent of the carbon positions. Generally, the paramagnetic orbital shift (δ_{para}) of the ^{13}C nucleus comprises contributions from the electronic excitations,²⁰⁾ $\langle \psi_i | L_z | \psi_j \rangle \langle \psi_j | L_z r^{-3} | \psi_i \rangle (E_j - E_i)^{-1}$, where L_z is the angular-momentum component along the external magnetic field, and i and j are the occupied and unoccupied electronic states, respectively. A possible explanation for the observed downfield shift is a small change in the average charge-transfer rate. If DAP is slightly more ionized in the low-resistance phase, the decreased π -electronic charge on DAP results in a decrease in the electron-electron repulsion, so that the reciprocal average distribution space ($\langle r^{-3} \rangle$) of the electron wavefunctions grows. Then, δ_{para} , which is roughly proportional to $\langle r^{-3} \rangle$ increases. Our estimate shows that the average $\Delta\delta$ (δ of the low-resistance phase minus δ of the pristine phase) 0.82 ppm can be explained by assuming a difference in the average charge-transfer rate between the two phases of as much as 0.6%. In an early study concerning the relationship between the ^{13}C chemical shift and the π -electron density of aromatic hydrocarbons, it was pointed out empirically that an upfield shift of 159.5 ppm takes place per one π -electron.²¹⁾ Our estimated value is also in good agreement with this empirical rule; our average downfield shift of 0.82 ppm corresponds to a 0.5% increase of charge transfer.

The observed small downfield shift can also be explained by the appearance of the electronic excited state level, because the transitions having small $E_j - E_i$ values contribute much to δ_{para} . The magnetic-susceptibility experiment suggests a low-lying electronic excited state for the low-resistance phase. It is impossible to quantitatively evaluate the contribution to ^{13}C δ_{para} from the excitation to this state, since the nature of this state is unknown. However, a significant contribution is expected if this excited state has some matrix elements with the occupied states. Our tentative estimate shows that the observed average shift of 0.82 ppm is explained by a 0.3% decrease in the average excitation energy.

Figure 9 shows the ^1H NMR spectra of pristine α -DAP-CHL and low-resistance α -DAP-CHL. The narrow line at 0 ppm comes from TTMS, an internal standard. Despite the fairly good resolution, amino and aromatic protons were not resolved in both phases, and even in pure DAP. It is, however, found that the proton signal for the low-resistance phase

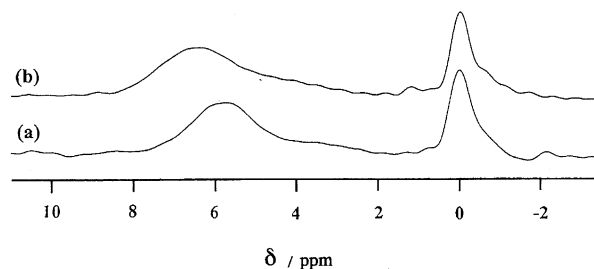
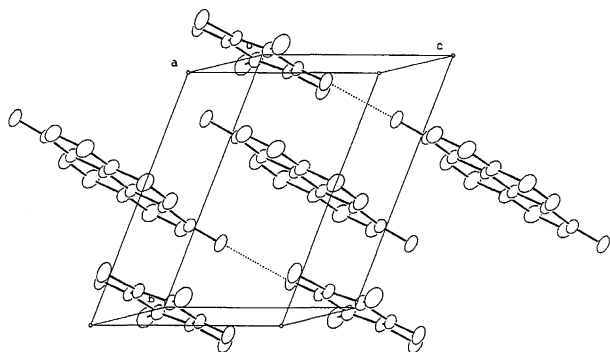


Fig. 9. Solid-state high resolution ^1H NMR spectra of pristine α -DAP-CHL (a) and low-resistance α -DAP-CHL (b). The signal at 0 ppm is due to an internal standard (TTMS).

exhibits a downfield shift of as much as 0.7 ppm relative to the signal for pristine α -DAP-CHL.

Summarizing the solid-state NMR results, both of the pristine and low-resistance phases of α -DAP-CHL comprise neutral DAP, and there is no detectable structural transformation between them. The small downfield shift of 0.5–1.0 ppm, compared with the pristine state observed in ^{13}C NMR, can be explained by an increased charge transfer of ca. 0.6%, or by a decrease in the average excitation energy of ca. 0.3% in the low-resistance phase. There is, however, an apparent discrepancy between the NMR and susceptibility measurements. The concentration of Curie spins obtained from the susceptibility measurements is expected to be sufficient to make the NMR lines much broader. The fairly narrow NMR lines in the low-resistance state shows that, if species bearing unpaired electrons are present, the electron spin states are flipping at a rate faster than MHz, or the electrons are delocalized. At the present stage, the conduction mechanism in the low-resistance state of α -DAP-CHL is not resolved. However, a key to understanding the mechanism will be that the low-resistance state is related to the very low-lying electronic excited state where the unpaired electrons do not contribute to NMR line broadening; this change in the electronic state does not accompany any appreciable structural change. In any case, it is highly likely that electrical conduction occurs in the mixed-stack complex with a neutral ground state. The conductivity is unusually high from both points of structure and electronic state of molecules. These facts suggest that there could be another conduction mechanism in which a charge carrier can travel in a crystal comprising neutral mixed-stacked molecules.

Crystal Structure of β -DAP-CHL. Another form obtained from the benzene solution, β -DAP-CHL, also has mixed-stacks of donors and acceptors, as shown in Fig. 10. The atomic parameters are summarized in Table 7. Compared with α -DAP-CHL, molecular overlapping between DAP and CHL in the stack, which is along the [011] direction, is insufficient. On the other hand, DAP is partly overlapped with another DAP in the neighboring column. The bond distances shown in Table 3 are not much different from those in α -DAP-CHL. When the geometry of CHL in β -DAP-CHL is compared with that in the CHL crystal or that in α -DAP-CHL (Table 4), it can be seen that CHL is neutral within the experimental error.

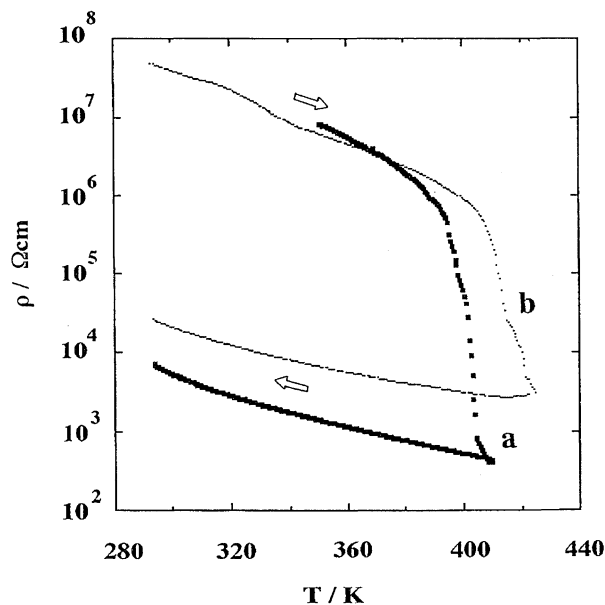
Fig. 10. Crystal structure of β -DAP-CHL.Table 7. Fractional Coordinates ($\times 10^4$) and Equivalent Temperature Factors for β -DAP-CHL

Atom	<i>x</i>	<i>y</i>	<i>z</i>	<i>B</i> _{eq} /Å ² a)
Cl(1)	-2453(1)	1553(1)	3024(1)	3.42(1)
Cl(2)	-3974(1)	684(1)	-2167(1)	3.47(1)
O(1)	-1342(2)	-964(2)	-4355(2)	3.01(4)
C(1)	-1169(2)	733(2)	1300(3)	2.25(4)
C(2)	-720(2)	-488(2)	-2382(2)	2.26(4)
C(3)	-1823(2)	330(2)	-889(3)	2.28(4)
N(1)	137(2)	2529(2)	-1599(2)	3.34(5)
C(4)	847(2)	3181(2)	631(3)	2.56(5)
C(5)	-236(2)	4025(2)	1982(2)	2.16(4)
C(6)	2067(2)	5655(2)	8868(3)	2.70(5)
C(7)	3066(2)	4850(2)	7532(3)	3.0(1)
C(8)	2347(2)	4292(2)	5207(3)	2.41(4)
C(9)	3367(2)	3483(2)	3799(3)	3.1(1)
C(10)	2639(3)	2939(2)	1568(3)	3.2(1)
C(11)	530(2)	4578(2)	4294(2)	1.94(4)

$$a) B_{eq} = 4/3 \sum_i \sum_j \beta_{ij} a_i \cdot a_j.$$

Electrical Resistivity of β -DAP-CHL. As expected from the neutral ground state of the complex and the mixed-stack-type structure, the crystal is an insulator with the resistivity of $10^8 \Omega \text{ cm}$ at room temperature. In contrast with α -DAP-CHL, the resistivity does not change when the crystals are transformed into a compressed pellet. With increasing the temperature, the resistivity of both the single crystal and compressed pellet undergoes a gradual decrease in addition to the normal decrease due to the thermal activation of semiconduction, as shown in Fig. 11. The temperature at which point the resistivity starts to decrease is much higher compared to the resistivity change of α -DAP-CHL. It can be noticed from Fig. 11 that the resistivity decrease is not smooth; the points where the decrease is stepwise correspond to where the temperature change rate is changed. Therefore, the process is slow at lower temperatures and is faster at higher temperatures. This observation suggests that this resistivity change is largely dominated by some kinetic process, such as chemical reactions. The lowest resistivity value achieved for β -DAP-CHL, 10^3 – $10^4 \Omega \text{ cm}$ at room temperature, is not as low as that for α -DAP-CHL.

It is most likely that the solid-state reaction making the resistivity low is a kind of ionization of molecules, since the

Fig. 11. Electrical resistivity change of β -DAP-CHL; single crystal **a**, and powder compaction **b**. Arrows are the direction of the temperature change.

ground state of this complex situates very close to the neutral–ionic boundary. In order to estimate the concentration of the ionized species, the ESR spectra of the low-resistance β -DAP-CHL compaction pellet were measured. The signal intensity of the sample is slightly stronger than that of low-resistance α -DAP-CHL, and the temperature dependence above 120 K is found to be roughly fitted by the Curie–Weiss type paramagnetism with a Weiss temperature of about -80 K . Since data at lower temperatures are required for estimating the exact parameter of the antiferromagnetic interaction, further analysis has not been tried. Though the apparent signal intensity is stronger than that of α -DAP-CHL, due to the much weaker antiferromagnetic interaction, the concentration of ionized species is found to be smaller than that found in low-resistance α -DAP-CHL; the estimated concentration is 1.7%. This value is again too small to be detected by the infrared spectra, and, indeed, the spectrum of low-resistance β -DAP-CHL was found to be almost the same as that of pristine β -DAP-CHL. Since the resistivity of low-resistance β -DAP-CHL is more than three-orders higher than that of low-resistance α -DAP-CHL, it is not unreasonable that only a part of the sample, which is ionized during the process, dominates the electrical conduction in β -DAP-CHL.

In conclusion, we have found that two polymorphs of DAP-CHL show an unusual electrical resistivity change upon heating; especially, the resistivity of low-resistance α -DAP-CHL is found to be as low as $10^0 \Omega \text{ cm}$. This is quite unusual, since the crystal of low-resistance α -DAP-CHL comprises mixed stacks of neutral donors and acceptors. Though a small portion of the ionized molecules detected by magnetic measurements is considered to be a key in the conduction process, no ordinary conduction mechanism can rationalize the low resistivity value. There might be another conduc-

tion mechanism in which charge carriers can travel in neutral mixed stacks of donors and acceptors. Since small conduction anisotropy in low-resistance α -DAP-CHL is observed, as found in DAP-TCNQ,⁹⁾ inter-stack transport through the hydrogen-bond could play some important role in this mechanism.

This work was partly supported by a Grant-in-Aid for Scientific Research No. 07454181 and on Priority Area No. 253 "Novel Electronic States in Molecular Conductors" from the Ministry of Education, Science and Culture, and by the Asahi Glass Foundation and the Iketani Science and Technology Foundation.

References

- 1) G. Saito and J. P. Ferraris, *Bull. Chem. Soc. Jpn.*, **53**, 2141 (1980).
- 2) J. B. Torrance, J. J. Mayerle, V. Y. Lee, and K. Bechgaard, *J. Am. Chem. Soc.*, **101**, 4747 (1979).
- 3) P. L. Kronick and M. M. Labes, *J. Chem. Phys.*, **35**, 2016 (1961).
- 4) P. L. Kronick, H. Scott, and M. M. Labes, *J. Chem. Phys.*, **40**, 890 (1964).
- 5) Y. Matsunaga, *Nature*, **205**, 72 (1965).
- 6) Y. Matsunaga, *Nature*, **211**, 183 (1966).
- 7) S. Koizumi and Y. Matsunaga, *Bull. Chem. Soc. Jpn.*, **45**, 423 (1972).
- 8) T. Inabe, *New J. Chem.*, **15**, 129 (1991).
- 9) T. Inabe, K. Okaniwa, H. Ogata, H. Okamoto, T. Mitani, and Y. Maruyama, *Acta Chim. Hung., -Models in Chem.*, **130**, 537 (1993).
- 10) H. Vollman, H. Becker, M. Corell, H. Streek, and G. Langbein, *Justus Liebigs Ann. Chem.*, **531**, 1 (1937).
- 11) Contamination of 1,8-diaminopyrene causes repeat defects along the [110] direction of the original α -form structure; T. Inabe and H. Goto, unpublished.
- 12) B. C. Gerstein and C. R. Dybowski, "Transient Techniques in NMR of Solids," Academic Press, New York (1985), Chaps. 5 and 6.
- 13) G. M. Sheldrick, "SHELX-86. Program for Crystal Structure Determination," University of Göttingen, Germany.
- 14) T. Sakurai and K. Kobayashi, *Rep. Inst. Phys. Chem. Res. (Jpn.)*, **55**, 69 (1979).
- 15) The lists of structure factors and anisotropic thermal parameters for non-hydrogen atoms are deposited as Document No. 69001 at the Office of the Editor of Bull. Chem. Soc. Jpn.
- 16) K. J. Van Weperen and G. J. Visser, *Acta Crystallogr., Sect. B*, **28**, 338 (1972).
- 17) G. Znotti and A. Del Pra, *Acta Crystallogr., Sect. B*, **36**, 313 (1980).
- 18) J. B. Torrance, J. E. Vazquez, J. J. Mayerle, and V. Y. Lee, *Phys. Rev. Lett.*, **46**, 253 (1981).
- 19) Since the α -DAP-CHL single crystal is not precisely parallelepiped, the exact direction of $\rho_{\perp c}$ is unknown. However, it has been confirmed that $\rho_{\perp c}$ always includes the component along the [221] direction (hydrogen-bonded direction), when the measurements were carried out in the most developed plane.
- 20) J. A. Pople, *J. Chem. Phys.*, **37**, 53 (1963); **37**, 60 (1963); M. Karplus and J. A. Pople, *J. Chem. Phys.*, **38**, 2803 (1963).
- 21) J. B. Stothers, "Carbon-13 NMR Spectroscopy," Academic Press, New York (1972), Chap. 3.